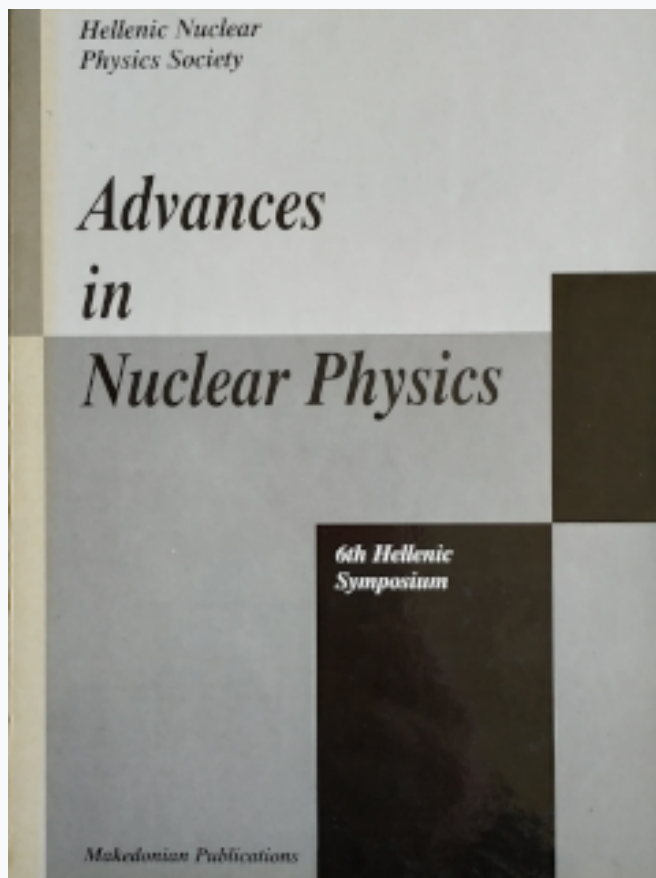


HNPS Advances in Nuclear Physics

Vol 6 (1995)

HNPS1995



Study of the Half-Diagonal Two-Body Density Matrix of Model Nuclear Matter

M. Petraki, E. Mavrommatis, J. W. Clark

doi: [10.12681/hnps.2916](https://doi.org/10.12681/hnps.2916)

To cite this article:

Petraki, M., Mavrommatis, E., & Clark, J. W. (2020). Study of the Half-Diagonal Two-Body Density Matrix of Model Nuclear Matter. *HNPS Advances in Nuclear Physics*, 6, 58–71. <https://doi.org/10.12681/hnps.2916>

Study of the Half-Diagonal Two-Body Density Matrix of Model Nuclear Matter

M. Petraki ^a, E. Mavrommatis ^{a,1}, and J. W. Clark ^b

^a *Physics Department, Division of Nuclear and Particle Physics, University of Athens, Panepistimiopoli, 15771 Athens, Greece*

^b *McDonnell Center for the Space Sciences and Department of Physics, Washington University, St. Louis, Mo 63130, USA*

Abstract

The half-diagonal two-body density matrix $\rho_{2h}(\mathbf{r}_1, \mathbf{r}_2, \mathbf{r}'_1)$ plays a central role in most theoretical treatments of the propagation of ejected nucleons and their final state interactions (FSI) in the nuclear medium. In this work based on the analysis of Ristig and Clark, we present the results of a Fermi hypernetted-chain calculation of $\rho_{2h}(\mathbf{r}_1, \mathbf{r}_2, \mathbf{r}'_1)$ for infinite symmetrical nuclear matter using a Jastrow-correlated model. The dependence of ρ_{2h} on the variables involved has been investigated in detail. Significant departures from ideal Fermi gas behavior in certain domains demonstrate the importance of short-range correlations. A comparison of our results with the predictions of Silver's approximation to ρ_{2h} , which has been employed in some treatments of FSI, reveals certain shortcomings of this approximation. The Fermi hypernetted-chain results obtained here will serve as a key input to an approximate treatment of FSI in inclusive quasielastic electron scattering from nuclear matter.

1 Introduction

In this paper we describe numerical calculations of the half-diagonal two-body density matrix $\rho_{2h}(\mathbf{r}_1, \mathbf{r}_2, \mathbf{r}'_1)$ of the ground state of uniform, isospin symmetrical, spin-saturated nuclear matter. The calculations have been performed within the framework of the microscopic analysis of ρ_{2h} carried out by Ristig and Clark [1] for a uniform strongly interacting Fermi fluid. The Ristig-Clark

¹ Presented by E. Mavrommatis

analysis implements correlated-basis-functions (CBF) theory at the variational level and involves hypernetted-chain techniques. The Fourier-space counterpart $n(\mathbf{p}, \mathbf{Q})$ of ρ_{2h} known as the generalized momentum distribution [1] has been the subject of a previous numerical study [2,3] based on the same analysis.

For a unit-normalized ground-state vector $|\Psi\rangle$, the half-diagonal two-body density matrix is defined by

$$\rho_{2h}(\mathbf{r}_1, \mathbf{r}_2, \mathbf{r}'_1) = A(A-1) \int \Psi^*(\mathbf{r}_1, \mathbf{r}_2, \mathbf{r}_3, \dots, \mathbf{r}_A) \cdot \Psi(\mathbf{r}'_1, \mathbf{r}_2, \mathbf{r}_3, \dots, \mathbf{r}_A) d\mathbf{r}_3 \dots d\mathbf{r}_A \quad (1)$$

In writing this expression, we have suppressed spin/isospin labels and a sum over all spin/isospin variables. The system is considered to have uniform nucleon density ρ with corresponding Fermi wave number $k_F = (6\pi^2\rho/\nu)^{1/3}$, where $\nu = 4$ is the level degeneracy of plane-wave single-particle states. Performing a Fourier transformation in the variables $\mathbf{r}_1 - \mathbf{r}'_1$ and $\mathbf{r}_1 - \mathbf{r}_2$, we obtain the generalized momentum distribution

$$n(\mathbf{p}, \mathbf{Q}) = \frac{1}{\nu} \frac{\rho}{A} \int \rho_{2h}(\mathbf{r}_1, \mathbf{r}_2, \mathbf{r}'_1) e^{-i\mathbf{p}\cdot(\mathbf{r}_1 - \mathbf{r}'_1)} e^{-i\mathbf{Q}\cdot(\mathbf{r}_1 - \mathbf{r}_2)} d\mathbf{r}_1 d\mathbf{r}_2 d\mathbf{r}'_1 \quad (2)$$

If we neglect dynamical correlations, the remaining kinematical correlations generated by the Pauli exclusion principle lead to the following half-diagonal two-body density matrix of the noninteracting system

$$\rho_{2h}^F(\mathbf{r}_1, \mathbf{r}_2, \mathbf{r}'_1) = \rho\rho_1^F(\mathbf{r}_1, \mathbf{r}'_1) - \frac{1}{\nu}\rho_1^F(\mathbf{r}_1, \mathbf{r}_2)\rho_1^F(\mathbf{r}'_1, \mathbf{r}_2) \quad (3)$$

where $\rho_1^F(\mathbf{r}_i, \mathbf{r}_j)$ is the one-body density matrix of the noninteracting Fermi gas,

$$\rho_1^F(\mathbf{r}_i, \mathbf{r}_j) = \rho l(k_F r_{ij}) \quad (4)$$

$l(x)$ being the Slater exchange function.

The half-diagonal two-body density matrix $\rho_{2h}(\mathbf{r}_1, \mathbf{r}_2, \mathbf{r}'_1)$ has several essential properties. First, it is a symmetric function of \mathbf{r}_1 and \mathbf{r}'_1 . Second, with our normalization choice, its diagonal part is connected to the radial distribution function $g(r_{12}) = g(|\mathbf{r}_1 - \mathbf{r}_2|)$ by

$$\rho_2(\mathbf{r}_1, \mathbf{r}_2, \mathbf{r}_1) = \rho^2 g(r_{12}) \quad (5)$$

Third, ρ_{2h} fulfills the sequential relation

$$\int \rho_{2h}(\mathbf{r}_1, \mathbf{r}_2, \mathbf{r}'_1) d\mathbf{r}_2 = (A-1)\rho_1(\mathbf{r}_1, \mathbf{r}'_1) \quad (6)$$

Fourth, if the system is subject to strong, short-range interparticle repulsions we must have

$$\rho_{2h}(\mathbf{r}_1, \mathbf{r}_1, \mathbf{r}'_1) = 0 \quad . \quad (7)$$

Finally, ρ_{2h} exhibits the following asymptotic properties:

$$\lim_{r_2 \rightarrow \infty} \rho_{2h}(\mathbf{r}_1, \mathbf{r}_2, \mathbf{r}'_1) = \rho \rho_1(\mathbf{r}_1, \mathbf{r}'_1) \quad , \quad (8)$$

$$\lim_{r'_1 \rightarrow \infty} \rho_{2h}(\mathbf{r}_1, \mathbf{r}_2, \mathbf{r}'_1) = \rho^2 g(r_{12}) \quad . \quad (9)$$

Several simple approximations have been proposed for estimating the half-diagonal two-body density matrix in uniform quantum fluids. In particular, Silver's approximation [4] expresses ρ_{2h} as a product of the one-body density matrix and the radial distribution function,

$$\rho_{2h}^S(\mathbf{r}_1, \mathbf{r}_2, \mathbf{r}'_1) \simeq \rho \rho_1(\mathbf{r}_1, \mathbf{r}'_1) g(|\mathbf{r}_1 - \mathbf{r}_2|) \quad . \quad (10)$$

It should be noted that this approximation is not symmetric in the variables \mathbf{r}_1 and \mathbf{r}'_1 . Gersch's approximation [5] uses the same basic ingredients (namely ρ_1 and g) in the form

$$\rho_{2h}^G(\mathbf{r}_1, \mathbf{r}_2, \mathbf{r}'_1) \simeq \rho \rho_1(\mathbf{r}_1, \mathbf{r}'_1) [g(|\mathbf{r}_1 - \mathbf{r}_2|)]^{1/2} [g(|\mathbf{r}'_1 - \mathbf{r}_2|)]^{1/2} \quad , \quad (11)$$

which violates the sequential relation (6). Rinat [6] has advocated the approximation

$$\rho_{2h}^R(\mathbf{r}_1, \mathbf{r}_2, \mathbf{r}'_1) \simeq \rho \rho_1(\mathbf{r}_1, \mathbf{r}'_1) g\left(\frac{1}{2}(\mathbf{r}_1 + \mathbf{r}'_1) - \mathbf{r}_2\right) \quad , \quad (12)$$

which violates the short-range property (7). Except as noted, these approximations fulfill the other formal properties of ρ_{2h} .

The diagonal part of ρ_{2h} , the two-particle distribution function $\rho^2 g(r_{12})$ of nuclear matter, is a fundamental descriptor of correlation structure that has been intensively studied in nuclear many-body theory [7]. Determination of the two-particle distribution function in finite nuclei is indirect, results being obtained recently for a few cases [8]. The 'full' half-diagonal two-body density matrix ρ_{2h} carries much richer information on the correlations existing in the nuclear medium. As in Bose systems [9], this quantity is expected to enter fundamental sum rules that furnish insights into the nature of the elementary excitations of nuclear matter. Moreover, it arises naturally in the description of a number of processes occurring in finite nuclei, notably in the calculation of dispersive effects in inelastic electron scattering [10]. However, the growing interest in ρ_{2h} has been driven by its appearance in quantitative 'post-mean-field' treatments of the propagation of ejected nucleons and their final state interactions (FSI). A proper treatment of FSI is critical to reliable extraction of

quantities like momentum distributions, spectral functions, and transparency from the results of experiments involving inclusive quasielastic (e, e') scattering [11], exclusive ($e, e'N$) scattering [12], proton scattering [13], pion absorption [14], etc.

Let us concentrate on inclusive quasielastic electron scattering at high energy E (several MeV to 1 GeV) and high momentum transfer q (on the order of several GeV/c) [11], for which empirical results exist for finite nuclei [15] and even for nuclear matter [16]. At low energy transfer ω , the cross section is sensitive to high-momentum components of the wave function, i.e., to short-range correlations, and also to the FSI of the recoiling nucleon within a spatial region of dimension $\sim 1/q$. The plane-wave impulse approximation generally underestimates the cross section at small ω [17]. FSI of the nucleon as it propagates within the correlated nuclear medium have been included in several theoretical approaches [18-24] to the quasielastic inclusive response of nuclear matter in the kinematic range under consideration. Specifically, two microscopic theories that have been used to calculate the relevant cross section are the correlated Glauber theory (CGT) [22,23], a generalization of Glauber theory that includes correlations, and the relativistic generalization of Gersch's theory (RGT) [24]. The half-diagonal two-body density matrix enters both theories; in CGT, it is evaluated by Silver's approximation [eq. (10)], and in RGT, by Gersch's approximation [eq. (11)]. In the GCT treatment, the results are found to be sensitive to the radial distribution function $g(r)$ employed. The two approaches overestimate the experimental cross section data at low ω by overestimating the FSI. Accordingly, these data have been taken as evidence for color transparency [25], a phenomenon predicted by pQCD that leads to a reduction of the FSI at high momentum transfer. Indeed, inclusion of this effect in the above treatments brings the derived results into good agreement with the data. However, such evidence for color transparency can be convincing only if the purely nucleonic FSI have been accurately evaluated. Among other improvements on the existing calculations, one should use a microscopically determined $\rho_{2h}(\mathbf{r}_1, \mathbf{r}_2, \mathbf{r}'_1)$ as input.

The first microscopic analyses of $n(\mathbf{p}, \mathbf{Q})$ and $\rho_{2h}(\mathbf{r}_1, \mathbf{r}_2, \mathbf{r}'_1)$ in strongly correlated systems were carried out by Ristig and Clark at the variational level of correlated-basis-function (CBF) theory, for both Bose and Fermi statistics [26,1]. Starting from cluster-diagrammatic decompositions of these quantities, Ristig and Clark applied hypernetted-chain techniques to their evaluation. In the present work, we report results of a Fermi hypernetted-chain treatment of $\rho_{2h}(\mathbf{r}_1, \mathbf{r}_2, \mathbf{r}'_1)$ in the leading approximation where elementary diagrams are omitted (FHNC/0). Section 2 gives a brief description of our calculational scheme. In Section 3, the numerical results for a simple nuclear matter model are presented and discussed. Finally, in Section 4, we state the main conclusions of our investigation and indicate the directions that will be taken in future work.

2 Fermi Hypernetted-Chain Calculation

The analysis, by Ristig and Clark [1], of the half-diagonal two-body density matrix ρ_{2h} of a uniform Fermi system is based on a Jastrow-Slater wave function. Development of the generalized momentum distribution $n(\mathbf{p}, \mathbf{Q})$ in a factorized Iwamoto-Yamada (FIY) cluster expansion leads, in the thermodynamic limit, to an infinite series whose addends are generally reducible, in that they are represented as products of cluster diagrams. Transformation to coordinate space yields the corresponding cluster series for ρ_{2h} . Resummation of the latter is then carried out, using hypernetted-chain techniques and taking into account asymptotic behaviors and relations to the Bose problem [26]. The function ρ_{2h} is expressed as a sum of two portions,

$$\rho_{2h}(\mathbf{r}_1, \mathbf{r}_2, \mathbf{r}'_1) = \rho_{2h}^{(2)}(\mathbf{r}_1, \mathbf{r}_2, \mathbf{r}'_1) + \rho_{2h}^{(3)}(\mathbf{r}_1, \mathbf{r}_2, \mathbf{r}'_1) \quad , \quad (13)$$

where $\rho_{2h}^{(2)}$ contains all terms generated purely by two-point functions and $\rho_{2h}^{(3)}$ is a remainder whose terms depend also on irreducible three-point functions. ('Two-point' and 'three-point' refer to the underlying graphical topology.) The first term, constructed from certain one-body density matrices and quantities given by solution of a set of FHNC equations, takes the explicit form

$$\begin{aligned} \rho_{2h}(\mathbf{r}_1, \mathbf{r}_2, \mathbf{r}'_1) = & \rho\rho_1(\mathbf{r}_1, \mathbf{r}'_1)g_{Qdd}(r)g_{Qdd}(r') + \\ & + \rho\rho_{1D}(\mathbf{r}_1, \mathbf{r}'_1)l(\mathbf{r}_1, \mathbf{r}'_1)[g_{Qdd}(r)F_{Qde}(r') + g_{Qdd}(r')F_{Qde}(r)] - \\ & - \nu\rho\rho_{1D}(\mathbf{r}_1, \mathbf{r}'_1)[\nu^{-1}l(r) - F_{Qcc}(r)][\nu^{-1}l(r') - F_{Qcc}(r')] \quad (14) \end{aligned}$$

The corresponding result for $\rho_{2h}^{(3)}$ may be found in ref. [1]. (The Q index appearing in eq. (14) is introduced to make the necessary connection with Ristig's notation [27]; it should not be confused with the momentum variable Q). In formula (14), $r = |\mathbf{r}_1 - \mathbf{r}_2|$ and $r' = |\mathbf{r}'_1 - \mathbf{r}_2|$. Further, $\rho_1(\mathbf{r}_1, \mathbf{r}'_1)$ is the full one-body density matrix, $\rho_{1D}(\mathbf{r}_1, \mathbf{r}'_1)$ is its direct-direct (dd) component, $F_{Qxy}(r)$ (with $xy = dd, de$ (direct-exchange), and cc (circular-circular)) are two-point quantities that serve as form factors, and $g_{Qdd}(r) - 1$ equals $F_{Qdd}(r)$. The FHNC result for ρ_{2h} is obtained by using results from FHNC evaluation of the one-body density matrix [27,28] and of the radial distribution function [4]. For example, one has $F_{Qxy}(r) = N_{Qxy}(r) + X_{Qxy}(r)$, where N_{Qxy} and X_{Qxy} are made up of the nodal (N) and non-nodal (X) diagrams that arise in the FHNC analysis of the one body-density matrix. Here we implement the FHNC algorithm at the initial (0th) level, where elementary diagrams are omitted, resulting in an FHNC/0 approximation. Contribution from elementary diagrams are expected to become important at densities higher than ordinarily found in nuclei [29]. We also omit the three-point quantity $\rho_{2h}^{(3)}$, since by similar reasoning it is expected to be small compared to the terms of $\rho_{2h}^{(2)}$. It turns out that our calculational scheme (the FHNC/0 algorithm together with omission

of $\rho_{2h}^{(3)}$) obeys the property (7) and preserves the symmetry in \mathbf{r}_1 and $\mathbf{r}_{1'}$, but is generally accompanied by (small) violations of the diagonal property (5) and the sequential relation (6). Henceforth, we shall refer to our calculational scheme as FHNC/0 for brevity.

3 Numerical results

The numerical results for the half-diagonal two-body density matrix are based on a simple model of nuclear matter near its saturation density, namely the ‘Monte Carlo’ (MC) model [30]. This model corresponds to the density value $\rho = 0.182 \text{ fm}^{-3}$ (or $k_F = 1.392 \text{ fm}^{-1}$) and is defined by the correlation function

$$f(r) = \exp \left[-C_1 e^{-C_2 r} \frac{(1 - e^{r/C_3})}{r} \right] \quad (\text{MC}) \quad (15)$$

with parameter values $C_1 = 1.7 \text{ fm}$, $C_2 = 1.6 \text{ fm}^{-1}$, and $C_3 = 0.1 \text{ fm}$. The MC model originated in a variational Monte Carlo treatment of the ground state of symmetrical nuclear matter based on the v_2 potential. The correlation function (15) describes the short-range correlations in a representative way and the intermediate and long-range correlations in an average way, but it misses the specific effects of the state dependence of the realistic nucleon-nucleon interaction. In Fig. 1, the radial distribution function $g(r)$ derived from our calculation with the MC model and FHNC/0 algorithm is compared with that obtained in ref. [22] for the Urbana v_{14} two-body interaction and the three-body force TNI . The MC model shows a ‘larger’ correlation hole than that produced by the v_{14} interaction. The MC model has the value 0.297 for the wound parameter $\kappa_{\text{dir}} = \rho \int (f(r) - 1)^2 dr$, which measures the strength of correlations. The MC model, along with the G2 model characterized by a κ_{dir} value of 0.111, have been used in our previous calculations of $n(\mathbf{p}, \mathbf{Q})$ [2,3].

We have studied the dependence of ρ_{2h} on the variables $r_{11'}$, r_{12} and $r_{1'2}$, considering the ranges $[0 - 10] \text{ fm}$ for $r_{11'}$ and $[0 - 5] \text{ fm}$ for r_{12} and $r_{1'2}$. In the two-dimensional plots of Figs. 2, 3, and 4, we present FHNC/0 results for the half-diagonal two-body density matrix at selected values of the three variables. For comparison, we include results for ρ_{2h} in the ideal Fermi gas and for ρ_{2h} derived from Silver’s approximation (10), along with the FHNC/0 results for $\rho_1(r_{11'})$ and $g(r_{12})$ corresponding to the MC model. In Fig. 2, $\rho_{2h}(\mathbf{r}_1, \mathbf{r}_2, \mathbf{r}'_1)$ is plotted as a function of r_{12} for three values of $r_{11'}$ (0.10, 1.93 and 3.76 fm). For each value of $r_{11'}$, three representative values of $r_{1'2}$ (0.10, 1.32 and 4.97 fm) have been chosen. In Fig. 3, $\rho_{2h}(\mathbf{r}_1, \mathbf{r}_2, \mathbf{r}'_1)$ is again displayed as a function of r_{12} , but now the results for the three chosen values of $r_{11'}$ are shown for each of the aforesaid values of $r_{1'2}$. Finally, Fig. 4 displays FHNC/0 results for $\rho_{2h}(\mathbf{r}_1, \mathbf{r}_2, \mathbf{r}'_1)$ as a function of $r_{11'}$ for three values of r_{12} (0.10, 1.32 and

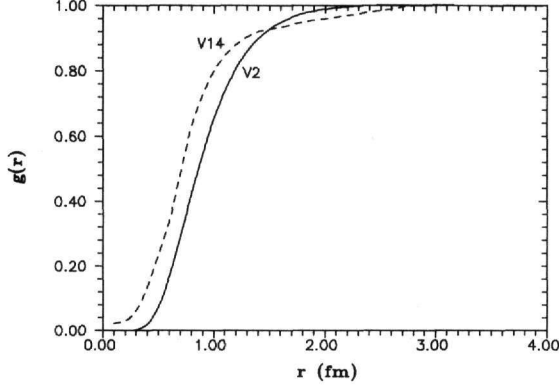


Fig. 1. Radial distribution function $g(r)$ as a function of r : (v_2) our calculation using MC model (eq. (15)) and the FHNC/0 algorithm, v_{14} variational calculation in ref. [22] using the Urbana v_{14} potential at $k_F = 1.33 \text{ fm}^{-1}$.

4.97 fm). For each value of r_{12} , the same three values of $r_{1'2}$ are adopted. Since $\rho_{2h}(\mathbf{r}_1, \mathbf{r}_2, \mathbf{r}'_1)$ is symmetric under interchange of r_{12} and $r_{1'2}$, further information on the behavior of this function may be inferred from the figures provided.

Generally $\rho_{2h}(\mathbf{r}_1, \mathbf{r}_2, \mathbf{r}'_1)$, viewed as a function of r_{12} for fixed values of $r_{11'}$ (less than 4.16 fm) and fixed values of $r_{1'2}$ (but not small), increases rapidly with increasing r_{12} , tending to the corresponding asymptotes. (For $r_{1'2} = 0.10 \text{ fm}$ this behavior cannot be distinguished for the scale employed in the figures.) Viewed as a function of $r_{11'}$ for fixed values of r_{12} and $r_{1'2}$, the quantity ρ_{2h} shows oscillatory behavior (although this is not visible for r_{12} or $r_{1'2}$ equal to 0.10 fm, again due to the scale chosen). It is found that these behaviors of $\rho_{2h}(\mathbf{r}_1, \mathbf{r}_2, \mathbf{r}'_1)$ are dictated mainly by the first term in the expression (14), namely $\rho\rho_1(\mathbf{r}_1, \mathbf{r}'_1)g_{Qdd}(r_{12})g_{Qdd}(r_{1'2})$, which is the dominant contribution under the stated conditions.

The impact of the dynamical correlations is revealed by comparing, in Figs. 2, 3, and 4, the curves derived from our FHNC/0 calculation with those corresponding to the noninteracting Fermi gas. Generally, correlations tend to lower the values of ρ_{2h} , this effect being quite significant. The calculated departures from the Fermi gas limit are larger for a given value of $r_{11'}$ and small [large] values of r_{12} , the larger [smaller] the values of $r_{1'2}$ are. For given values of r_{12} and $r_{1'2}$, a significant effect of correlations on ρ_{2h} as a function of $r_{11'}$ is to shift the oscillations of ρ_{2h} to smaller values of $r_{11'}$. (Due to the scale used, this effect is not evident in Fig. 4 for $r_{12} = 0.10 \text{ fm}$ and the three values of $r_{1'2}$ considered, nor for $r_{12} = 1.32 \text{ fm}$ or 4.97 fm and $r_{1'2} = 0.10 \text{ fm}$.)

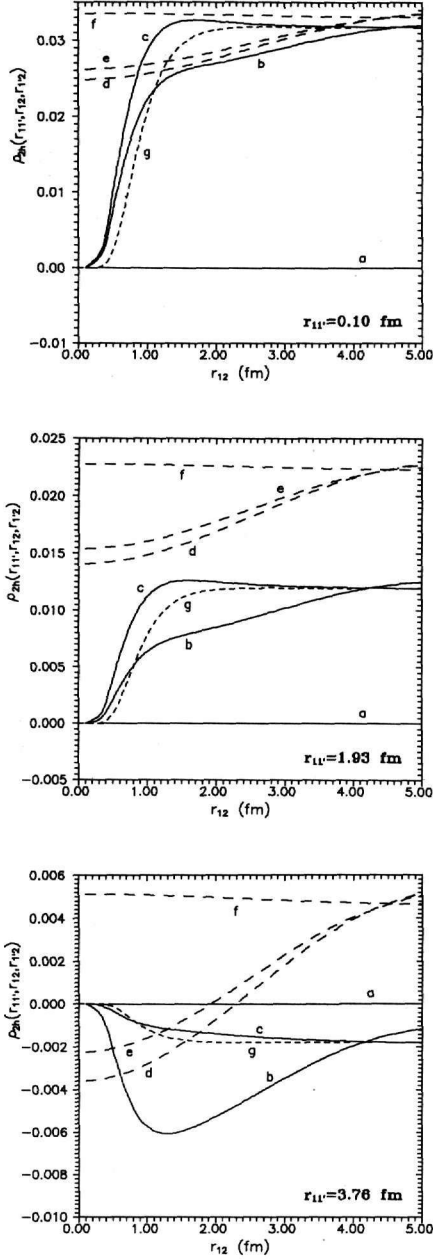


Fig. 2. Half-diagonal two-body density matrix $\rho_{2h}(r_1, r_2, r'_1)$ at nucleon density $\rho = 0.182 \text{ fm}^{-3}$ as a function of r_{12} for constant values of r_{11}' (equal to 0.10 fm, 1.93 fm and 3.76 fm) and of $r_{1'2}$ (equal to 0.10 fm (curves (a), (d)), 1.32 fm (curves (b), (e)) and 4.97 fm (curves (c), (f))). Long-dashed line: ideal Fermi gas, continuous line: FHNC/0 calculation, and short-dashed line: Silver's approximation. The last two are calculated with MC correlations (eq. (15)).

Figs. 2, 3, and 4 provide for a comparison of our results (denoted by $\rho_{2h}^{FHNC/0}$) with those obtained with Silver's approximation (denoted by ρ_{2h}^S). It is to be noted that the approximation ρ_{2h}^S does not depend on $r_{1'2}$. At given $r_{11'}$, the difference between ρ_{2h}^S and $\rho_{2h}^{FHNC/0}$, as a function of r_{12} , depends on the value of $r_{1'2}$ considered. For small values of $r_{1'2}$, there are large deviations for almost all values of r_{12} (except the small ones). For intermediate values of $r_{1'2}$, the approximations ρ_{2h}^S and $\rho_{2h}^{FHNC/0}$ almost coincide at small r_{12} ; at intermediate values of r_{12} , the discrepancy is larger (and almost independent of $r_{11'}$); and at large r_{12} the two approximations are again almost coincident. For large values of $r_{1'2}$, it is found that ρ_{2h}^S and $\rho_{2h}^{FHNC/0}$ nearly coincide at small r_{12} ; at intermediate values of r_{12} , they show significant differences (though to a smaller extent than in the preceding case); and at large r_{12} the two evaluations are again in agreement. A further assessment of the validity of Silver's approximation can be made using Fig. 5, in which the two approximations that are used to form ρ_{2h}^S , specifically

$$\rho_1(r_{11'}) \approx \rho_{1D}(r_{11'})l(r_{11'}), \quad (16)$$

$$F_{Qdd}(r_{12}) + F_{Qde}(r_{12}) \approx g(r_{12}) - 1, \quad (17)$$

are plotted and compared with the respective left-hand sides computed via FHNC/0. The deficiencies of Silver's estimate are evident from these comparisons and speak for the advisability of using $\rho_{2h}^{FHNC/0}$ rather than ρ_{2h}^S (for example) in the treatment of FSI within correlated Glauber theory [22,23]. Thereby one may be able to draw more convincing conclusions from experiment regarding the quantitative importance of nuclear and color transparency in inclusive quasielastic scattering of GeV electrons off nuclear matter at high momentum transfers. In addition to Silver's estimate, Gersch's approximation ρ_{2h}^G [eq. (11)] has been applied in this problem [24]. We have found ρ_{2h}^G to provide a generally better approximation to $\rho_{2h}^{FHNC/0}$ than is given by ρ_{2h}^S [31]. It will be interesting to determine the quantitative effect of using $\rho_{2h}^{FHNC/0}$ in the treatment of FSI developed in ref. [24].

4 Conclusions

In summary, we have presented a microscopic evaluation, within Fermi hypernetted-chain theory, of the half-diagonal two-body density matrix $\rho_{2h}(\mathbf{r}_1, \mathbf{r}_2, \mathbf{r}'_1)$ of nuclear matter, for the case of state-independent, central, two-body correlations. The momentum-space transform $n(\mathbf{p}, \mathbf{Q})$ of ρ_{2h} has been calculated previously within the same framework [2,3]. Our results for $\rho_{2h}(\mathbf{r}_1, \mathbf{r}_2, \mathbf{r}'_1)$ demonstrate a rich sensitivity of this observable to short range-correlations. They also exhibit significant departures from the results given by Silver's approximation [4] in certain regions of the variables involved. These differences

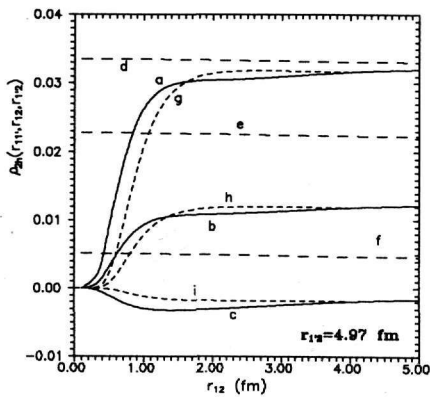
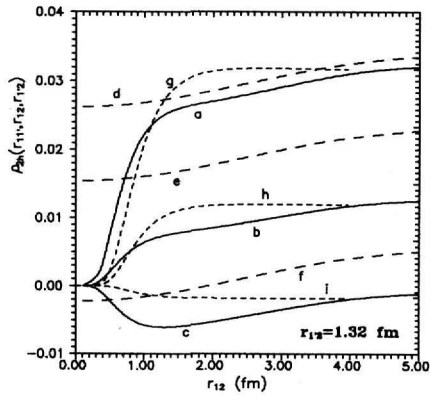
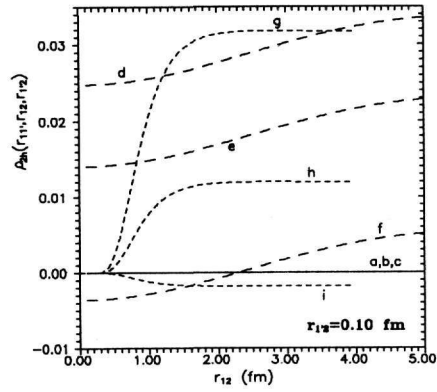


Fig. 3. As in Fig. 2 but with the use of the constant values of r_{11}' and r_{12}' reversed. Curves (g), (h) and (i): Silver's approximation for r_{11}' equal to 0.10 fm, 1.93 fm and 3.76 fm respectively.

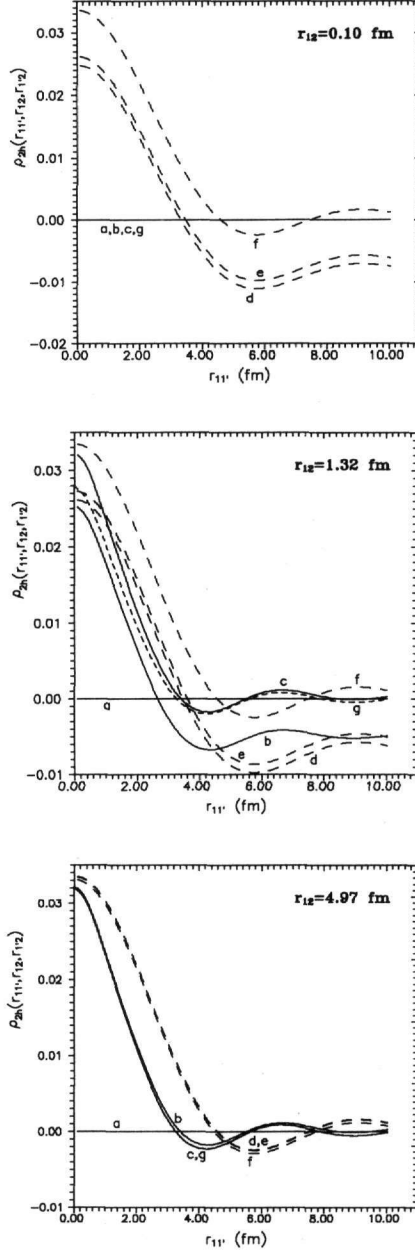


Fig. 4. Half-diagonal two-body density matrix $\rho_{2h}(r_1, r_2, r_1')$ at nucleon density $\rho = 0.182 \text{ fm}^{-3}$ as a function of r_{11}' for constant values of r_{12} and of r_{12}' (equal to 0.10 fm (curves (a), (d)), 1.32 fm (curves (b), (e)) and 4.97 fm (curves (c), (f))). Long-dashed line: ideal Fermi gas, continuous line: FHNC/0 calculation and short-dashed line: Silver's approximation. The last two are calculated with MC correlations (eq. (15)).

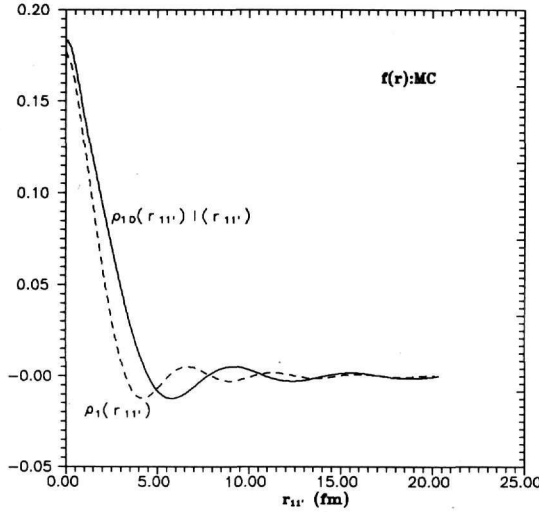
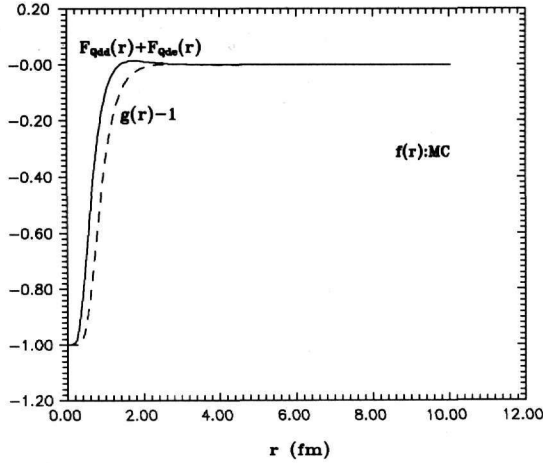


Fig. 5. Comparison of FHNC/0 results for the quantities $F_{Qdd}(r) + F_{Qde}(r)$ and $g(r) - 1$ as well as $\rho_1(r_{11'})$ and $\rho_{1D}(r_{11'})l(r_{11'})$ computed for the MC $f(r)$ and $\rho = 0.182 \text{ fm}^{-3}$. Here $F_{Qdd}(r)$ and $F_{Qde}(r)$ are form factors entering expression (14), $\rho_1(r_{11'})$ and $\rho_{1D}(r_{11'})$ are the full one-body density matrix and its direct-direct part respectively and $l(r_{11'})$ the Slater exchange function.

are expected to have significant repercussions within existing treatments of final-state interactions. The FHNC/0 results we have generated for ρ_{2h} will be employed as input to a description of FSI in inclusive quasielastic scattering of GeV electrons from nuclear matter, based on correlated Glauber theory [23]. Further investigations of $\rho_{2h}(\mathbf{r}_1, \mathbf{r}_2, \mathbf{r}'_1)$ in nuclear matter should extend the available analysis and the calculations to realistic, state-dependent correlations. There has recently been some progress toward this goal within

self-consistent Green's function theory [32]. However, it can be argued that our results obtained with central state-independent correlations should be reasonable in the problem of (e, e') quasielastic scattering at high momentum and small energy transfers, where short-range repulsive correlations are dominant. With regard to microscopic determination of $\rho_{2h}(\mathbf{r}_1, \mathbf{r}_2, \mathbf{r}'_1)$ for finite nuclei, a local-density-approximation might be developed, as has been done for the one-body density matrix in refs. [33,34].

Acknowledgements

We acknowledge financial support by the Greek Secretariat of Research and Development under Contract No. 360/91 and by the U.S. National Foundation under Grant No. PHY-9307484. A preliminary version of this work was presented at the Conference 'Perspectives of Nuclear Physics at Intermediate Energies,' Trieste, May 1995. E. M thanks the Organizers for their kind hospitality.

References

- [1] M. L. Ristig and J. W. Clark, Phys. Rev. B **41** (1990) 8811.
- [2] J. W. Clark, E. Mavrommatis, and M. Petraki, Acta. Phys. Pol. **24** (1993) 659 [Janusz Dabrowski Festschrift Issue].
- [3] E. Mavrommatis, M. Petraki and J. W. Clark, Phys. Rev. C **51** (1995) 1849.
- [4] R. N. Silver, Phys. Rev. B **38** (1988) 2283.
- [5] H. A. Gersch, L. J. Rodriguez, and P. N. Smith, Phys. Rev. A **5**, (1972) 1547.
- [6] A. S. Rinat, Phys. Rev. B **40** (1989) 6625.
- [7] J. W. Clark, in *Progress in Particle and Nuclear Physics*, Vol. 2, edited by D. H. Wilkinson (Pergamon Press, Oxford, 1979), p. 89.
- [8] D. H. Beck, Phys. Rev. Lett. **64** (1990) 268.
- [9] S. Stringari, Phys. Rev. B **46** (1992) 2974.
- [10] E. A. J. M. Offermann, L. S. Cardman, H. J. Enrich, G. Fricke, C. W. de Jager, H. Miska, D. Rychel, and H. de Vries, Phys. Rev. Lett. **57** (1986) 1546.
- [11] I. Sick, Prog. Part. Nucl. Phys. **34** (1995) 323 and references therein.
- [12] L. Lapikás, Nucl. Phys. **A553** (1993) 297c and references therein.

- [13] A. S. Carroll, D. S. Barton, G. Bunce, S. Gushue, Y. I. Makdisi, S. Heppelmann, H. Courant, G. Fang, K. J. Heller, M. L. Marshak, M. A. Shupe, and J. J. Russel, *Phys. Rev. Lett.* **61** (1988) 1698.
- [14] D. Ashery and J. P. Schiffer, *Ann. Rev. Nucl. Part. Sci.* **36** (1986) 207.
- [15] D. B. Day, J. S. McCarthy, Z. E. Meziani, R. Minehart, R. M. Sealock, S. T. Thornton, J. Jourdan, I. Sick, B. W. Filippone, R. D. McKeown, R. G. Milner, D. H. Potterveld, and Z. Szalata, *Phys. Rev. Lett.* **59** (1987) 427; *Phys. Rev. C* **48** (1993) 1849.
- [16] D. B. Day, J. S. McCarthy, Z. E. Meziani, R. Minehart, R. M. Sealock, S. T. Thornton, J. Jourdan, I. Sick, B. W. Filippone, R. D. McKeown, R. G. Milner, D. H. Potterveld, and Z. Szalata, *Phys. Rev. C* **40** (1989) 1011.
- [17] C. Ciofi degli Atti, E. Pace, and G. Salmè, *Phys. Rev. C* **43** (1991) 1155.
- [18] S. A. Gurvitz and A. S. Rinat, *Phys. Lett. B* **197** (1987) 6.
- [19] T. Uchiyama, A. E. L. Dieperink, and O. Scholten, *Phys. Lett. B* **233** (1989) 31.
- [20] J. W. Clark and R. N. Silver, in *Proceedings of the Fifth International Conference on Nuclear Reaction Mechanisms*, edited by E. Gadioli (Università degli Studi di Milano, 1988), p. 531.
- [21] M. N. Butler and S. E. Koonin, *Phys. Lett. B* **205** (1988) 123.
- [22] O. Benhar, A. Fabrocini, S. Fantoni, G. A. Miller, V. R. Pandharipande, and I. Sick, *Phys. Rev. C* **44** (1991) 2328.
- [23] O. Benhar, A. Fabrocini, S. Fantoni, V. R. Pandharipande, S. C. Pieper, and I. Sick, *Phys. Lett. B* **359** (1995) 8.
- [24] A. S. Rinat and M. F. Taragin, *Nucl. Phys. A* **571** (1994) 733; preprint WIS-95/11/Mar-PH, to appear in *Nucl. Phys. A*.
- [25] L. L. Frankfurt and M. I. Strikman, *Phys. Rep.* **160** (1988) 235 and references therein.
- [26] M. L. Ristig and J. W. Clark, *Phys. Rev. B* **40** (1989) 4355.
- [27] M. L. Ristig, in *From Nuclei to Particles*, Proceedings of the International School of Physics "Enrico Fermi," Course LXXIX, Varenna, 1980, edited by A. Molinari (North-Holland, Amsterdam, 1982), p. 340.
- [28] S. Fantoni, *Nuovo Cimento A* **44** (1978) 191.
- [29] V. R. Pandharipande and R. B. Wiringa, *Rev. Mod. Phys.* **51** (1979) 821.
- [30] D. Ceperley, G. V. Chester, and M. H. Kalos, *Phys. Rev. B* **16** (1977) 3081.
- [31] M. Petraki, E. Mavrommatis, and J. W. Clark, in preparation.
- [32] C. C. Gearhart, Ph.D. Thesis, Washington University, St. Louis, 1994.
- [33] S. Stringari, M. Traini, and O. Bohigas, *Nucl. Phys. A* **516** (1990) 33.
- [34] G. Cò, A. Fabrocini, and S. Fantoni, *Nucl. Phys. A* **568** (1994) 73.